

Characterization and catalytic properties of zeolite MCM-22

R. Ravishankar, D. Bhattacharya, N.E. Jacob, S. Sivasanker *

National Chemical Laboratory, Pune 411 008, India

Received 5 September 1994; accepted 24 October 1994

Abstract

Characterization of MCM-22 was carried out by X-ray diffraction (XRD), scanning electron microscopy (SEM), thermal analysis (TGA–DTA) and nuclear magnetic resonance (NMR). TGA–DTA and NMR studies indicate a strong interaction of the template with the zeolite framework. Adsorption studies indicate the internal void volume to be intermediate between the volumes of zeolite beta and ZSM-12. In catalytic reactions such as the isomerization of *m*-xylene, aromatization of *n*-hexane and transformation of methanol to hydrocarbons, the zeolite behaves like a large-pore zeolite, even though recent research has established that it is a medium-pore zeolite.

Keywords: MCM-22; Characterization of MCM-22; Synthesis of MCM-22; Catalytic properties of MCM-22; Medium-pore zeolites; high-silica zeolites

1. Introduction

The zeolites PSH-3, SSZ-25 and MCM-22, synthesized and patented by three different groups, are believed to possess similar structures [1–3]. Interestingly, a large number of patents claim the use of MCM-22 in reactions normally carried out over both medium- and large-pore zeolites [4–6]. The structure of MCM-22 was reported only recently [7], even though PSH-3 was patented in 1984. Leonowicz et al. [7] supposed that the zeolite possessed two independent pore systems, that were both accessed through 10-membered rings. One of the pore systems was defined by two-dimensional sinusoidal channels. The other consisted of large supercages with an inner free diameter of 7.1 Å, 12-membered rings, and an inner height of 18.2 Å; the supercages were interlinked through double 6-rings. A number of publications have appeared very recently in the literature on the synthesis and

catalytic properties of this zeolite [8–12]. However, to date, no detailed physicochemical studies have been reported. In this paper, we report more information on the physicochemical and catalytic properties of MCM-22.

The zeolite has been characterized by techniques such as XRD, SEM, TGA–DTA, Fourier transform infrared (FTIR) and magic-angle spinning (MAS) NMR as well as by adsorption studies. Catalytic reactions such as the isomerization of *m*-xylene, aromatization of *n*-hexane and transformation of methanol have also been carried out.

2. Experimental

2.1. Zeolite synthesis

Samples of MCM-22 with different SiO₂/Al₂O₃ ratios were prepared based on procedures described elsewhere [3,8]. A typical synthesis for

* Corresponding author.

obtaining a zeolite with a $\text{SiO}_2/\text{Al}_2\text{O}_3$ ratio of about 30 is described below.

Sodium silicate [43.58 g; Lona Industries, Bombay, India; composition (w/w): 26.69% SiO_2 , 9.10% Na_2O , 64.11% H_2O] was mixed with distilled water (20 g) in a polypropylene beaker (250 ml capacity). Hexamethylenimine (8.81 g; Aldrich; 99% purity) was added dropwise over a period of 30 min to the above sodium silicate solution under vigorous stirring using a mechanical stirrer (SS 316 blades). The pale yellow mixture was stirred for a further 15 min. Then a solution of aluminium sulfate (4.33 g; $\text{Al}_2(\text{SO}_4)_3 \cdot 18\text{H}_2\text{O}$; Merck, Bombay, India) and concentrated sulfuric acid (3.52 g; 98 wt.-%; Ranbaxy Labs., Punjab, India) in distilled water (110 g) was added slowly over a period of 15 min with vigorous stirring. Stirring was continued for 1 h. The mixture was pale yellow, turbid and had a pH of 11.4. The composition of the above mixture in terms of oxide mole ratio was 9.83 Na_2O :29.78 SiO_2 : Al_2O_3 :13.70 R:1367.9 H_2O .

The mixture was then transferred to an autoclave (300 ml capacity; SS 316, Parr Instruments, USA). The sealed autoclave was heated to 423 K under stirring (250 rpm) and kept at that temperature for 80 h. At the end of the 80 h, the autoclave was lifted from the heater and cooled rapidly by immersion in cold water. The white crystalline product which was separated from the mother liquor (pH 12.4) by filtration using a Buchner funnel was washed well with distilled water.

The washed material was dried at 393 K for 6 h. The XRD pattern of the material confirmed it to be pure MCM-22. The template was removed by calcining first in a flow of nitrogen at 723 K for 4 h and then in dry air at 823 K for 6 h. The yield of the calcined sample (on dry basis) was 92% of theoretical. The zeolite was analyzed for chemical composition using wet chemical methods: it had a $\text{SiO}_2/\text{Al}_2\text{O}_3$ ratio of 28. It was next ion-exchanged with a 1 M solution of ammonium acetate thrice at 360 K (10 ml of solution for 1 g of solid; duration of each exchange was 6 h). The NH_4^+ -exchanged zeolite was filtered through a Buchner funnel and thoroughly washed with distilled water. The sample was dried at 393 K for 6 h and calcined in dry air at 773 K for 6 h.

2.2. XRD studies

Powder XRD data for the as-synthesized and calcined samples of the zeolite were collected on a computer-automated diffractometer (Model D-MAX III VC, Rigaku, Japan). The materials were ground and dried first at 383 K for 2 h. These samples were equilibrated over a saturated CaCl_2 solution at room temperature for 6 h prior to measurements. They were then packed on a glass sample holder. Nickel-filtered $\text{CuK}\alpha$ radiation was used with a graphite monochromator. Data were collected in the 2θ range of 4–50° with a step size of 0.02° and a step time of 10 s with continuous rotation of the sample during the scan. Silicon was used as the internal standard.

2.3. Sorption measurements

Argon adsorption measurements were carried out using a commercial volumetric adsorption apparatus (Model Omnisorp 100CX, Coulter, USA). About 200 mg of the calcined sample were degassed at 675 K and $\sim 10^{-5}$ Torr prior to adsorption measurements. Hydrocarbon adsorption data were obtained using a vacuum microbalance (Cahn Instruments, USA). Again, the samples were degassed at 675 K for 12 h at $\sim 10^{-5}$ Torr prior to sorption measurements. The measurements were carried out at 298 K at a P/P_0 of 0.5. Uptake was measured for 2 h. Adsorption equilibria were reached within this period for all hydrocarbons studied.

2.4. FTIR studies

Samples were mixed with KBr and self-supported KBr pellets were used. FTIR spectra were recorded in a Nicolet 60 SX B FTIR spectrometer.

2.5. Thermal measurements

TGA–DTA analysis of an as-synthesized sample ($\text{SiO}_2/\text{Al}_2\text{O}_3 = 28$) was carried out in air and helium in the temperature range 298–1173 K (temperature program rate of 10 K/min; Model 92-12 instru-

ment, Setaram, France). The temperature-programmed decomposition–desorption (TPD) of the as-synthesized sample in argon was carried out in a separate apparatus (Sorbstar, Institute of Isotopes, Hungary). The output was analyzed with a TCD cell and a quadrupole mass spectrometer (Hilden, UK).

2.6. Catalytic studies

The H form of the zeolite was used. The zeolite powder was compacted and broken into particles (12–18 mesh). Normally, 1.5 g of the catalyst were loaded in a vertical down flow reactor (glass) with an I.D. of 10 mm. The feed was injected using a syringe pump (Sage Instruments, USA or Braun, Germany). AR methanol (Qualigens, India; >98% purity, further distilled), *m*-xylene (Aldrich, USA; >99% purity) and *n*-hexane, (S.D. Fine Chemicals, India; >99% purity) were used. The catalyst was dried at 753 K in a flow of dry nitrogen prior to carrying out the reaction under the desired conditions. The gaseous and liquid products were analyzed by gas chromatography using a capillary column (HP1; cross-linked methyl silicone gum; 50 m × 0.2 mm; Hewlett Packard Model 5990 A gas chromatograph) and a packed column (Carbowax; 2 m × 3 mm; Shimadzu Model 15 gas chromatograph).

3. Results and discussion

3.1. Scanning electron microscopy

The SEM photograph of the as-synthesized MCM-22 ($\text{SiO}_2/\text{Al}_2\text{O}_3=28$) is shown in Fig. 1. The crystals are mostly platelets of approximately 1–2 μm diameter and 0.1–0.2 μm thickness bunched into 4–5 μm particles. Calcination of the samples did not affect the morphology of the crystals. Samples with other $\text{SiO}_2/\text{Al}_2\text{O}_3$ ratios (58 and 88) had a similar crystal morphology.

3.2. X-Ray diffraction

The XRD lines for MCM-22 (calcined sample; $\text{SiO}_2/\text{Al}_2\text{O}_3=28$) are presented in Table 1 along with those for MCM-22, PSH-3 and SSZ-25. The correspondence of many lines with the reported



Fig. 1. Scanning electron micrograph of MCM-22 ($\text{SiO}_2/\text{Al}_2\text{O}_3=28$).

values [13] indicates that all materials possess similar structures. Our analysis of the X-ray lines also shows that MCM-22 is different from FU-1, though some common lines are present [14]. The X-ray patterns for the sample before and after calcination are presented in Fig. 2a and b, respectively. The two patterns are similar except for changes in the intensities of some peaks. The general broadness of the peaks (Fig. 2) could be due to the presence of stacking faults or to the platelets being made up of microcrystallites.

3.3. Thermal analyses

The TGA–DTA and TPD plots are presented in Fig. 3a–c. Adsorbed water is lost from the zeolite up to about 423 K (Fig. 3b and c). After this, template loss occurs in two steps in both helium (c) and air (b), the steps being below and above 753 K. In the case of helium, the weight loss amounts to a total of 10.8% in steps of 6.9 and 3.9%. In air, the template weight loss is 8.9% in steps of 3.2 and 5.7%. The decomposition of the template (hexamethylenimine) in inert atmosphere occurs at temperatures below 753 K into small C fragments like CH_4 , C_2H_4 , C_3H_6 and NH_3 (Fig. 3a). The hydrocarbon fragments account for a loss of 6.9%. As these (especially NH_3 and CH_4) are richer in H_2 than the parent compound, a C-rich skeleton remains on the zeolite and desorbs at a much higher temperature.

Mass spectral data also reveal that very little

Table 1
Comparison of X-ray powder diffraction data of synthesized sample with MCM-22, PSH-3 and SSZ-25

Laboratory sample (SiO ₂ /Al ₂ O ₃ =28)		Literature [13] [d (nm) and relative intensities]					
d (nm)	I/I ₀	MCM-22		PSH-3		SSZ-25	
—	—	3.000	(w-m)	—	—	—	—
—	—	2.210	(w)	—	—	2.550	(17)
1.229	40	1.236	(m-vs)	1.263	(vs)	1.230	(100)
1.106	26	1.103	(m-s)	1.092	(m)	1.100	(55)
0.882	34	0.886	(w-m)	0.884	(vs)	0.878	(63)
0.685	11	—	—	0.686	(w)	—	—
0.615	44	0.618	(m-vs)	0.615	(s)	0.617	(40)
0.600	17	0.600	(w-m)	—	—	—	—
0.552	17	0.554	(w-m)	0.550	(w)	0.551	(17)
—	—	—	—	0.492	(w)	0.491	(w)
0.467	5	0.464	(w)	0.460	(w)	—	—
0.455	5	—	—	—	—	—	—
0.440	16	0.441	(w-m)	0.439	(w)	—	—
0.408	23	0.425	(w)	—	—	—	—
—	—	0.410	(w-s)	0.409	(w)	—	—
0.405	32	0.406	(w-s)	—	—	—	—
0.391	48	0.391	(m-vs)	0.391	(m)	0.390	(38)
0.375	24	0.375	(w-m)	0.375	(w)	—	—
0.356	20	0.356	(w-m)	0.356	(w)	—	—
0.352	13	—	—	—	—	0.347	(20)
0.342	100	0.342	(vs)	0.341	(vs)	0.342	(65)
0.330	24	0.330	(w-m)	0.330	(w-m)	—	—
0.320	20	0.320	(w-m)	0.319	(w)	—	—
—	—	0.314	(w-m)	0.311	(w)	—	—
—	—	0.299	(w)	—	—	—	—
0.283	7	0.282	(w)	0.283	(w)	—	—
0.282	7	—	—	—	—	—	—
0.277	7	0.278	(w)	—	—	—	—
0.268	13	0.268	(w)	0.269	(w)	—	—

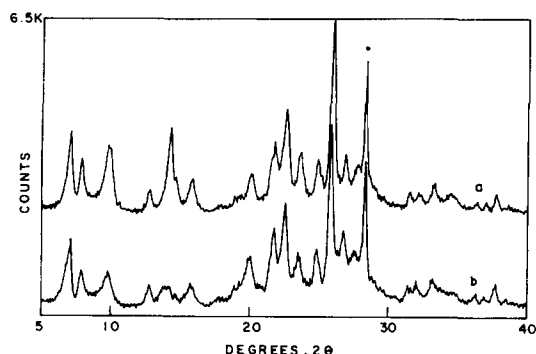


Fig. 2. XRD patterns for MCM-22(SiO₂/Al₂O₃=28): (a) as-synthesized sample; (b) calcined sample; Si line marked by a dot.

undecomposed template is desorbed. An intriguing aspect of the TGA-DTA experiments is the exothermic nature of the template loss in helium. The same template decomposed endothermally in the case of the molecular sieves AlPO₄-5 and AlPO₄-22. Rough calculations point out that the exothermicity of the peak cannot be accounted for from differences in heats of formation of the template and the hydrocarbon fragments. Both the exothermicity and greater weight loss in helium can be explained if we assume that partial oxidation of the template (especially H) by the surface -OH groups occurs during its decomposition. In air, the combustion of the H part of the template is rapid, so loss of most of the H and N atoms occurs below 753 K (3.2%), the rest of

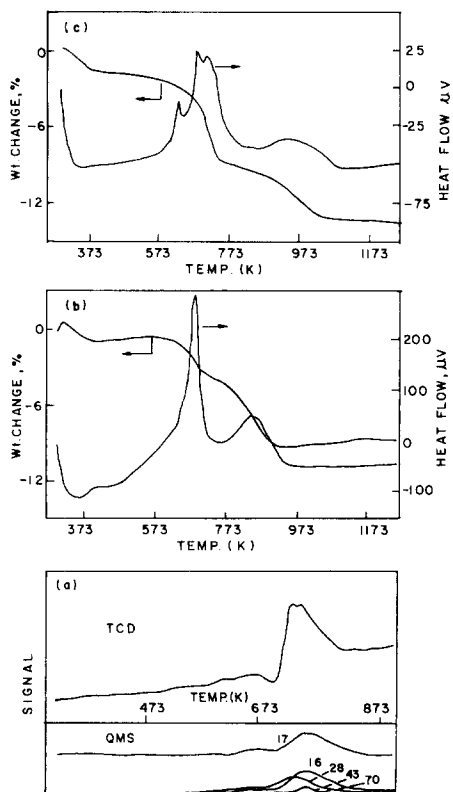


Fig. 3. TGA-DTA and TPD of as-synthesized MCM-22 ($\text{SiO}_2/\text{Al}_2\text{O}_3 = 28$): (a) TPD of template; (b) TGA-DTA in air; (c) TGA-DTA in helium.

the C-skeleton burning at a higher temperature (850 K). The fragmentation of the template during desorption even in helium and the two-step combustion of the molecule in air indicate that the template is very strongly held inside the zeolite pores. The C, H and N microanalyses of the same sample also indicated that the template constitutes $\approx 10\%$ of the as-synthesized sample.

The above results (Fig. 3) suggest that at least a part of the template is more strongly adsorbed than the rest. The template could be present in two types of locations: inside the 10-membered ring channels (strong interaction) and inside the 12-membered ring cages (weaker interaction).

3.4. Magic-angle spinning nuclear magnetic resonance

The NMR spectra were recorded with an MSL 300 Bruker Fourier transform NMR instru-

ment following standard methods described elsewhere [15]. In order to examine the extent of interaction of the template (hexamethyleneimine, Fig. 4a) with the zeolite, the ^{13}C NMR spectra of the neat liquid template, the template adsorbed (9 wt.-%) over SiO_2 gel (S5505, Sigma) and the as-synthesized sample were recorded (Fig. 4b–d, respectively). The spectrum of liquid hexamethyleneimine (Fig. 4b) shows three sharp lines: at $\delta = 27.60$, 31.95 and 49.74 ppm for the three non-equivalent pairs of C atoms, viz. C-3–C-4, C-2–C-5 and C-1–C-6, respectively. Two broad lines were observed for the template (9 wt.-%) adsorbed on SiO_2 -gel at $\delta = 27.6$ and 56.26 ppm (Fig. 4c). In the case of the as-synthesized MCM-22, the

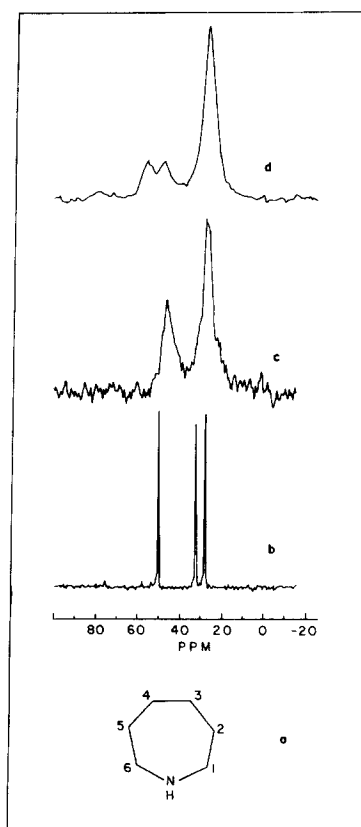


Fig. 4. ^{13}C NMR spectra of the template molecule in different environments: (a) the template molecule, hexamethyleneimine; (b) spectrum of hexamethyleneimine (liquid); (c) spectrum of hexamethyleneimine adsorbed on SiO_2 gel; (d) spectrum of as-synthesized MCM-22 ($\text{SiO}_2/\text{Al}_2\text{O}_3 = 88$); NMR reference: adamantane, CH, $\delta = 37.8$ ppm.

spectrum was similar to that of the SiO_2 gel sample except that the low-field signal was split into a doublet with $\delta=47.53$ and 55.62 ppm (Fig. 4d). The results reveal the non-equivalence in the magnetic environment of the C-1 and C-6 atoms when the molecule is located inside the pores of the zeolite. This confirms the strong interaction of the template with the zeolite framework.

The ^{27}Al MAS NMR spectrum of the calcined samples with $\text{SiO}_2/\text{Al}_2\text{O}_3$ ratios of 57 and 88 consisted of a single line at $\delta=57.58$ and 57.84 ppm, respectively, showing the presence of tetrahedral aluminium only. However, a weak signal at $\delta=2.19$ ppm corresponding to octahedral Al^{3+} ions was noticed in the case of the sample with $\text{SiO}_2/\text{Al}_2\text{O}_3=28$, whose intensity was $<3\%$ of the total Al^{3+} signal in the sample. The ^{29}Si spectrum was well resolved in the case of the sample with $\text{SiO}_2/\text{Al}_2\text{O}_3=88$ and consisted of five lines at $\delta=-99.39$, -103.67 , -110.69 , -113.28 and -119.71 ppm. The signal at $\delta=-99.39$ ppm is due to $\text{Si}(1\text{Al})$, while the others correspond to $\text{Si}(0\text{Al})$ and $\text{Si}(\text{OH})$ groups. In the case of the samples with lower $\text{SiO}_2/\text{Al}_2\text{O}_3$ ratios, the ^{29}Si signals were less well resolved and an additional signal corresponding to $\text{Si}(2\text{Al})$ was also identified.

3.5. Framework infrared spectra

The framework infrared spectrum (Fig. 5) of MCM-22 (calcined; $\text{SiO}_2/\text{Al}_2\text{O}_3=28$) exhibits the characteristic features of zeolites [16]. The prominent bands are attributable to the different internal tetrahedral and external linkage vibrations. Based on Flanigen [16], the prominent bands have been assigned as follows:

1245 cm^{-1}	external linkages; asymmetric stretching
1080 cm^{-1}	internal tetrahedra; asymmetric stretching
835 cm^{-1}	external linkages; symmetric stretching
725 cm^{-1}	internal tetrahedra; symmetric stretching
610 and 555 cm^{-1}	external linkages; double ring

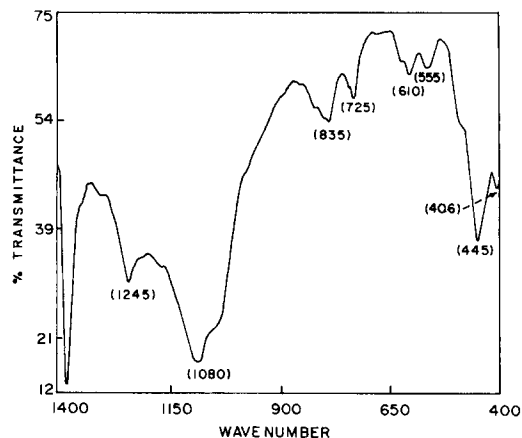


Fig. 5. Framework IR spectrum of MCM-22 ($\text{SiO}_2/\text{Al}_2\text{O}_3=28$).

445 cm^{-1}	internal tetrahedra; T-O bend
406 cm^{-1}	pore-opening (12-membered ring?)

In the case of dealuminated Y, Flanigen [16] assigned the bands in the region of $402\text{--}408\text{ cm}^{-1}$ to 12-membered ring pore opening. The occurrence of a weak band at 406 cm^{-1} in MCM-22 suggests the presence of 12-membered aluminosilicate rings.

3.6. Sorption characteristics

Studies of the sorption of Ar , H_2O and hydrocarbons were carried out over the H form of the samples. The results obtained on a typical sample ($\text{SiO}_2/\text{Al}_2\text{O}_3=28$) are presented in Table 2 and Fig. 6.

Comparative sorption data obtained over a number of other zeolites are also presented in Table 2. The micropore volume of MCM-22 is larger than that of ZSM-5, a typical medium-pore zeolite with a two-dimensional pore system. The pore volume (0.20 ml/g) is between that of ZSM-12 (a large-pore zeolite with a one-dimensional pore system) and that of beta (a large-pore zeolite with a three-dimensional pore system). The pore size, 0.7 nm , measured by the Horvath-Kawazoe method [17] is also similar to that of mordenite (0.72 nm). The corresponding values for ZSM-5 and H-Y are 0.64 and 0.72 nm , respectively. The

Table 2
Studies on the sorption characteristics of zeolites

Zeolite	SiO ₂ /Al ₂ O ₃ ratio	N ₂ adsorption ^a		Sorbed at $P/P_0=0.5$ (wt.-%)			Pore system; size (nm)	Source
		Micropore volume (ml/g)	S_{BET} (m ² /g)	H ₂ O (0.265 nm) ^b	<i>n</i> -Hexane (0.43 nm) ^b	1,3,5-TMB (0.84 nm)		
ZSM-5	39	0.13	413	7.7	13.5	0.5	2D; 0.54 × 0.56, 0.51 × 0.55	UCIL, India
ZSM-12	81	0.17	465	9.2	8.3	2.6	1D; 0.57 × 0.6	Synthesized as per Ref. [22]
Beta	35	0.28	600	20.1	15.9	17.0	3D; 0.75 & 0.55	PQ, Netherlands
Mordenite	44	0.25	568	17.5	11.4	7.0	1D; 0.67 × 0.7	Norton, USA
H-Y	5.2	0.34	820	—	20.9	24.0	3D; 0.74; cages, 1.3	Linde, USA
MCM-22	28	0.20	505	15.0	11.5	8.5	Unknown	Synthesized as per Ref. [8]

^a Argon adsorption in the case of MCM-22 and mordenite.

^b Values in parentheses are the kinetic diameters of the molecules [23] or the critical diameter in the case of 1,3,5-TMB [24].

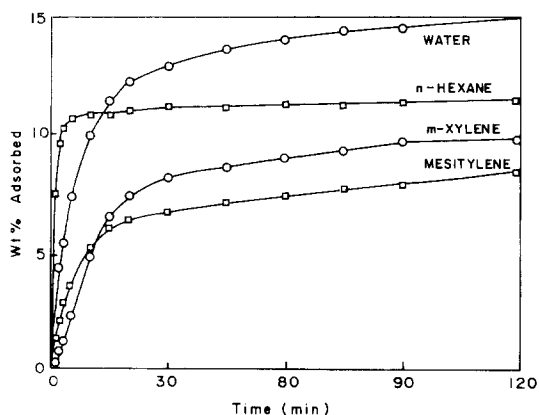


Fig. 6. Sorption isotherms of probe molecules over MCM-22 (SiO₂/Al₂O₃=28); temperature=298 K; $P/P_0=0.5$.

total BET surface area of the calcined sample (SiO₂/Al₂O₃=28) was 505 m²/g. The external surface area measured on the as-synthesized material filled with the template was 60 m²/g. Mesitylene (1,3,5-trimethylbenzene, 1,3,5-TMB) adsorption was rapid (70% adsorption occurring in 15 min) and large (8.5 wt.-%) in the case of MCM-22. The corresponding mesitylene adsorption values for ZSM-5 and ZSM-12 were 0.5 and 2.6%.

3.7. Catalytic activity measurements

m-Xylene isomerization

The isomerization of *m*-xylene is an acid-catalyzed reaction and takes readily place over the H form of MCM-22. The influence of contact time on the isomerization of *m*-xylene over MCM-22 is presented in Table 3. Earlier workers have shown that, when diffusion effects are absent, the probabilities of producing the *p*- and *o*-isomers are nearly equal and the *p/o* ratio of xylenes in the product does not depend on the acid strength of the zeolite [18]. Hence, the important parameter affecting the *p*-xylene/*o*-xylene ratio is the diffusion selectivity. Dewing [19] reported that the diffusivity ratios of *p*-xylene to *o*-xylene (D_{para}/D_{ortho}) were 12.82 and 1.73 in the case of ZSM-5 (medium pore; ~0.55 nm) and mordenite (large pore; ~0.67 nm) at 673 K. The *p/o* ratio of the xylenes in the reaction product is usually between 1 to 1.2 (close to the equilibrium value of 1.1) in the case of large-pore zeolites and above 2 in the case of medium-pore zeolites [18]. The *p/o* ratio in the case of MCM-22 was found to be 1.1 ± 0.1 (Table 3), similar to the values normally observed for large-pore zeolites.

Table 3
Influence of WHSV on isomerization of *m*-xylene over MCM-22^a

Compound	Products (% w/w)				
	1.76 h ⁻¹	3.47 h ⁻¹	6.5 h ⁻¹	8.68 h ⁻¹	13.02 h ⁻¹
Conversion (% w/w)	58.1	39.7	20.2	9.5	4.1
Benzene	1.13	1.21	0.54	0.35	0.34
Toluene	2.90	2.42	1.70	1.35	0.85
<i>m</i> -Xylene	41.87	60.35	79.77	90.5	95.91
<i>p</i> -Xylene	16.08	12.42	5.43	2.16	1.10
<i>o</i> -Xylene	15.54	12.20	5.10	2.02	1.27
1,3,5-TMB	6.28	2.97	1.54	0.57	0.08
1,2,4-TMB	14.45	7.57	5.14	2.27	0.42
1,2,3-TMB	1.71	0.90	0.63	0.27	0.02
<i>p</i> -Xylene/ <i>o</i> -xylene	1.03	1.02	1.06	1.07	0.87
Log (I/D)	0.22	0.33	0.50	0.55	0.60
1,3,5-TMB/1,2,4-TMB	0.43	0.39	0.29	0.25	0.18

^a Reaction conditions: feed, *m*-xylene/hydrogen (1:4, mol/mol); temperature = 573 K; time on stream (TOS), 2 h.

The isomerization of *m*-xylene is invariably accompanied by disproportionation reactions (to toluene and trimethylbenzenes) over acid zeolites. Disproportionation of *m*-xylene is a bimolecular reaction and involves the formation of bulkier 1,1-diphenylmethane intermediates inside the pore system [18].

The yield of a particular trimethylbenzene in the product will depend on the availability of void space inside the zeolite to accommodate the specific intermediate; the intermediate leading to 1,3,5-TMB is bulkier than the ones leading to 1,2,4-TMB or 1,2,3-TMB. The void space in different zeolites can therefore be estimated (in a relative sense) by comparing the ratios of the 1,3,5- and 1,2,4-TMB isomers in the product at similar conversions. A higher value will indicate a larger available void space. The 1,3,5-TMB/1,2,4-TMB ratios for beta, mordenite and ZSM-12 are 0.36, 0.16 and 0.08, respectively, at 623 K at a conversion level of 10% [20]. The values reported by Martens et al. [18] are 0.30 for MOR, 0.30 for BEA and 0.0 for MTW at conversions between 6.9 and 10.6% at a temperature of 623 K. The 1,3,5-TMB/1,2,4-TMB ratio observed over MCM-22 at a 9.5% conversion and 573 K is 0.25 (Table 3). In addition to the 1,3,5-TMB/1,2,4-TMB values, the ratio of products formed

by isomerization (I) to those formed by disproportionation (D) during *m*-xylene isomerization can also be used to gauge the void space in the zeolites [18]; low I/D ratios will imply the availability of a large void volume in the zeolite, wherein bimolecular disproportionation reactions can occur. The value of log(I/D) extrapolated to zero conversion has been used to rank zeolites according to their void space [21]. The value of log(I/D) obtained at zero conversion for MCM-22 is 0.66 (Table 3), while it is 0.9 for BEA, 1.2 for MOR and 1.8 for MTW [20].

n-Hexane conversion

n-Hexane cracks readily over acid zeolites to produce lighter hydrocarbons, the major products being C₃, C₄ and C₂ compounds. Above 723 K, the cracked products oligomerize to yield aromatics. The formation of aromatics is especially significant over the medium-pore zeolites of the high-silica type such as ZSM-5 and ZSM-11, the aromatization reaction presumably being assisted by the medium-sized pores (5–6 Å) in these zeolites. The results of the aromatization of *n*-hexane over MCM-22 are presented in Table 4. For comparison, the results obtained over ZSM-5 have also been presented. The major observation is that,

Table 4
Aromatization of *n*-hexane over MCM-22 and ZSM-5^a

Parameter	MCM-22 (2.5 h ⁻¹)		ZSM-5 (798 K)	
	773 K	798 K	41.0 h ⁻¹	2.3 h ⁻¹
Conversion of <i>n</i> -hexane (% w/w)	59.95	63.41	61.95	100
Products (% w/w)				
C ₁	1.17	1.57	1.10	11.31
C ₂	10.14	12.82	8.84	15.79
C ₃	26.77	28.84	27.75	36.29
C ₄	9.94	10.01	9.18	3.89
C ₅ + aliphatics	44.29	40.42	49.22	0.27
Benzene	0.34	0.55	0.82	8.06
Toluene	0.84	0.95	2.73	13.09
Ethylbenzene	0.08	0.05	0.24	0.57
<i>m</i> -Xylene	0.49	0.50	1.26	3.75
<i>p</i> -Xylene	0.25	0.17	0.71	0.91
<i>o</i> -Xylene	0.23	0.16	0.55	1.52
C ₈ + aromatics	0.43	0.48	0.87	4.16
Σ aromatics	2.66	2.86	7.17	32.06
<i>p</i> -Xylene/ <i>o</i> -xylene	1.09	1.06	1.29	0.66

^a Reaction condition: feed: *n*-hexane/hydrogen (1:1.5, mol/mol); TOS, 4 h.

at the same conversion level, MCM-22 produces much fewer aromatics than ZSM-5.

Transformation of methanol to hydrocarbons

The effects of temperature and space velocity (WHSV) on the transformation of methanol over MCM-22 were studied (Tables 5 and 6). For comparative purposes, the reactions were also carried out over ZSM-5 and BETA (Table 7).

At temperatures below 573 K, only C₂–C₅ hydrocarbons are produced over MCM-22 (Table 5). The yield of heavier aromatics reaches a maximum at 573 K and decreases at higher temperatures. The production of heavier aromatics like tetramethyl-, pentamethyl- and hexamethylbenzenes suggests that the pore system is large enough to permit their formation [25–29].

The results of the WHSV studies are presented in Table 6. The production of heavier aromatics is large at WHSV=1.0 h⁻¹, but decreases slowly with increase in space velocity.

The reaction was carried out under identical

Table 5
Effect of temperature on conversion of methanol^a

	Products (% w/w)				
	373 K	473 K	573 K	643 K	673 K
Conversion (%)	10.08	72.25	85.04	87.66	92.72
C ₁ + C ₂	–	–	1.51	2.54	4.60
C ₃	–	0.17	3.97	8.30	13.29
C ₄	99.39	99.83	63.42	68.18	51.70
C ₅ + aliphatics	0.61	–	10.69	12.13	20.35
C ₆ –C ₈ aromatics	–	–	0.44	0.56	0.33
>C ₈ aromatics ^b	–	–	19.97	8.28	9.74

^a Reaction conditions: WHSV, 1.0 h⁻¹; catalyst, 1.5 g; N₂/methanol, 1.5 (mol/mol); TOS, 1 h.

^b >C₈ aromatics correspond to ≥95% hexamethylbenzene and ≤5% to pentamethylbenzene and durene.

conditions over a medium-pore zeolite (MFI) and a large-pore zeolite (BEA) (Table 7). It was found that over ZSM-5 the conversion was 100% and there was no production of heavier aromatics. The yield of C₆–C₈ aromatics was found to be more over ZSM-5 [30]. In the case of the other two zeolites, MCM-22 and BETA, conversion was around 95%; the formation of polymethylbenzenes (>C₈ aromatics) was significant and that of C₆–C₈ aromatics was small. Polymethylbenzenes, especially hexamethylbenzenes (kinetic diameter of 0.75 nm), are formed in large-pore zeolites only [25–29].

4. Conclusion

MCM-22 has been shown to contain large 12-membered ring cages, accessible only through 10-membered ring openings [7]. In the reactions reported above, however, it behaves like a wide-pore (12-membered ring) zeolite. Even adsorption data suggest that it could be a wide-pore zeolite. Some workers [10–12] have observed that it behaves both as a 10-membered ring and as a 12-membered ring zeolite in different reactions. The observations can be explained in the following manner: (1) the zeolite has a large external area (due to platelet structure) and a significant number of reactions occur on the external surface; (2) there

Table 6
Influence of WHSV on the conversion of methanol over MCM-22^a

	Products (% w/w)					
	0.5 h ⁻¹	1.0 h ⁻¹	2.55 h ⁻¹	5.0 h ⁻¹	7.5 h ⁻¹	10.0 h ⁻¹
Conversion (%)	97.08	95.76	93.96	87.66	85.51	83.33
C ₁ +C ₂	10.26	6.77	7.15	2.54	7.61	3.25
C ₃	17.32	16.13	14.17	8.3	21.7	9.46
C ₄	38.5	36.18	52.16	68.18	44.21	69.59
C ₅ +aliphatics	19.68	18.36	19.27	12.13	16.58	12.28
C ₆ –C ₈ aromatics	0.08	0.31	0.19	0.56	0.36	0.47
>C ₈ aromatics ^b	14.17	22.27	7.08	8.28	9.59	4.96

^a Reaction conditions: temperature, 643 K; N₂/methanol, 1.5 (mol/mol); TOS, 1 h.

^b >C₈ aromatics correspond to ≥95% hexamethylbenzene and ≤5% to pentamethylbenzene and durene.

Table 7
Methanol conversion over ZSM-5, MCM-22, BETA, mordenite and USY: a comparative study^a

	Products (% w/w)				
	H-ZSM-5	H-MCM-22	H-BETA	H-MORD [25]	USY [26]
Conversion (%)	100	95.8	95.5	–	–
C ₁ +C ₂	6.4	6.8	21.4	17.8	–
C ₃	33.7	16.1	19.1	21.6	–
C ₄	21.8	36.2	31.2	23.6	–
C ₅ +aliphatics	18.2	18.3	20.8	18.6	–
C ₆ –C ₈ aromatics	14.8	0.3	0.3	2.3	–
>C ₈ aromatics ^b	5.1 ^c	22.3 ^d	7.2 ^d	18.1 ^d	100 ^b

^a Reaction conditions: temperature, 643 K; WHSV, 1.0 h⁻¹; N₂/methanol, 1.5 (mol/mol); TOS, 1 h.

^b >C₈ corresponds to pure hexamethylbenzene in this case.

^c In this case, [ZSM-5], >C₈ aromatics corresponds to trimethyl- and tetramethylbenzenes only.

^d >C₈ aromatics corresponds to hexamethylbenzene (≥95%) and pentamethylbenzene and durene (≤5%).

are cracks and mesopores in the platelet crystallites which access the 12-membered ring cages directly; (3) the 12-membered ring cages may open out at the external surface wherever there are stacking faults.

Acknowledgements

R.R. and D.B. thank UGC (New Delhi, India) for senior research fellowships.

References

- [1] L. Puppe and J. Weisser, *US Pat.*, 4439409 (1984).
- [2] S.I. Zones, *Eur. Pat. Appl.*, EP 231 019 (1987).
- [3] M.K. Rubin and P. Chu, *US Pat.* 4954325 (1990).
- [4] R.P.L. Absil, S. Han, D.O. Marler and D.S. Shihabi, *US Pat.* 4962257 (1990).
- [5] C.T.W. Chu, T.F. Degnan and B.K. Huh, *US Pat.*, 4982033 (1991).
- [6] G.W. Kirker, S. Mirzahi and S.S. Shih, *US Pat.*, 5000839 (1991).
- [7] M.E. Leonowicz, J.A. Lawton, S.L. Lawton and M.K. Rubin, *Science*, 264 (1994) 1910.
- [8] R. Ravishankar, Tapas Sen, Veda Ramaswamy, H.S.

- Soni, S. Ganapathy and S. Sivasanker, *Stud. Surf. Sci. Catal.*, 84(A) (1994) 331.
- [9] S. Unverricht, M. Hunger, S. Ernst, H.G. Karge and J. Weitkamp, *Stud. Surf. Sci. Catal.*, 84(A) (1994) 37.
- [10] A. Corma, C. Corell, A. Martinez and J. Pèrez-Pariente, *Stud. Surf. Sci. Catal.*, 84(A) (1994) 859.
- [11] A. Corma, C. Corell, F. Llopis, A. Martinez and J. Pèrez-Pariente, *Appl. Catal. A: General*, 115 (1994) 121.
- [12] W. Souverijns, W. Verrelst, G. Vanbutsele, J.A. Martens and P.A. Jacobs, *J. Chem. Soc. Chem. Commun.*, (1994) 1671.
- [13] R. Szostak, *Handbook of Molecular Sieves*, Van Nostrand Reinhold, New York, NY, 1991.
- [14] J. Dewing, M.S. Spencer and T.V. Whittam, *Catal. Rev. Sci. Eng.*, 27 (1985) 461.
- [15] A. Thangaraj, R. Kumar and P. Ratnasamy, *Zeolites*, 11 (1991) 573.
- [16] E.M. Flanigen, *Am. Chem. Soc. Monogr.*, 171 (1976) Ch. 2.
- [17] G. Horvarth and K. Kawazoe, *J. Chem. Soc. Jpn.*, 16 (1983) 470.
- [18] J.A. Martens, J. Perez-Pariente, E. Sastre, A. Corma and P.A. Jacobs, *Appl. Catal.*, 45 (1988) 85.
- [19] J. Dewing, *J. Mol. Catal.*, 27 (1984) 25.
- [20] R. Kumar and K.R. Reddy, *Microporous Mater.*, in press.
- [21] R. Kumar, G.N. Rao and P. Ratnasamy, *Stud. Surf. Sci. Catal.*, 49(B) (1989) 1141.
- [22] S. Ernst, P.A. Jacobs, J.A. Martens and J. Weitkamp, *Zeolites*, 7 (1986) 25.
- [23] D.W. Breck, *Zeolite Molecular Sieves*, Wiley-Interscience, New York, NY, 1974.
- [24] P.E. Eberly, *Am. Chem. Soc. Monogr.*, 171 (1976) Ch. 7.
- [25] C.D. Chang, *Hydrocarbons from Methanol*, Marcel Dekker, New York, NY, 1983.
- [26] B. Sulikowski and A. Popielarz, *Appl. Catal.*, 42 (1988) 251.
- [27] M. Sawa, M. Niwa and Y. Murakami, *Chem. Lett.*, 8 (1987) 1630.
- [28] P. Salvador and W. Kladnig, *J. Chem. Soc., Faraday I*, (1977) 1153.
- [29] O.V. Kikhtyanin, V.M. Mastikhin and K.G. Ione, *Appl. Catal.*, 42 (1988) 1.
- [30] C.D. Chang and A.J. Silvestri, *J. Catal.*, 47 (1977) 249.